

LA-UR-17-20513

Approved for public release; distribution is unlimited.

Title: Emissivity Measurements of Additively Manufactured Materials

Author(s): Morgan, Robert Vaughn
Reid, Robert Stowers
Baker, Andrew M.
Lucero, Briana
Bernardin, John David

Intended for: Report

Issued: 2017-01-25

Disclaimer:

Los Alamos National Laboratory, an affirmative action/equal opportunity employer, is operated by the Los Alamos National Security, LLC for the National Nuclear Security Administration of the U.S. Department of Energy under contract DE-AC52-06NA25396. By approving this article, the publisher recognizes that the U.S. Government retains nonexclusive, royalty-free license to publish or reproduce the published form of this contribution, or to allow others to do so, for U.S. Government purposes. Los Alamos National Laboratory requests that the publisher identify this article as work performed under the auspices of the U.S. Department of Energy. Los Alamos National Laboratory strongly supports academic freedom and a researcher's right to publish; as an institution, however, the Laboratory does not endorse the viewpoint of a publication or guarantee its technical correctness.

Emissivity Measurements of Additively Manufactured Materials

Preliminary Report

11/09/2016

Robert Morgan, Robert Reid, Andrew Baker, Briana Lucero, and John Bernardin

Contents

Figures.....	1
Tables.....	1
Abstract.....	2
Introduction.....	2
Apparatus.....	3
Procedure.....	4
Results.....	4
Conclusions.....	8
References.....	8
Appendix A.....	9

Figures

Figure 1. Variation of emissivity with angle for typical conductors (e.g. metals) and non-conductors (e.g. plastics) (Incropera & DeWitt, 2002).	3
Figure 2. Infrared images of a sample at 0, 20, 50, and 80 angular degrees (from left to right).....	4
Figure 3. Raw apparent temperature measurements versus angle for each emissivity sample coupon....	6
Figure 4. Change in apparent temperature measurements to eliminate contribution of initial temperature on data profiles.	7
Figure 5. Emissivity calculated by setting the 0 degree value to that from Table 2, then adjusting the emissivity at the remaining angles until the temperature matches. This technique is easily influenced by temperature fluctuations.....	7

Tables

Table 1. Emissivity values for various common engineering materials. Note that the metals (conductors) have very low emissivity values, while the plastics (non-conductors) have high emissivity values. Values are normal emissivity from Infrared Training Center, 2015, whereas *the value of Teflon is total hemispherical emissivity from Incropera & DeWitt, 2002.	3
Table 2. Emissivities measured using the Gier- Dunkle reflectometer (Reid, 2016).	5
Table 3. Orientation key to number descriptors for sample coupons.....	5

Abstract

The emissivity of common 3D printing materials such as ABS and PLA were measured using a reflectivity meter and have the measured value of approximately 0.92. Adding a conductive material to the filament appears to cause a decrease in the emissivity of the surface. The angular dependence of the emissivity and the apparent temperature was measured using a FLIR infrared camera showing that the emissivity does not change much for shallow angles less than 40 angular degrees, and drops off dramatically after 70 angular degrees.

Introduction

For the purpose of constructing numerical thermal models for additively manufactured parts, the emissivity of the part characterizes the contribution to the energy balance of emitted and absorbed radiation. Additionally, this value is useful for the measurement of surface temperatures using infrared (FLIR) cameras, where emissivity is required to correct received radiation to temperature. This property is most generally a function of angle, temperature, wavelength, and surface treatment. Therefore, measurements of emissivity at test conditions represent the most accurate values available. Herein we will present emissivity measurements for a number of common additive manufacturing materials, and will attempt to measure the angular dependence of the emissivity for these materials.

For an object at a steady temperature, the radiation energy balance for a surface can be expressed simply as

$$a + r + t = 1,$$

where a is the absorptivity, r is the reflectivity, and t is the transmissivity (Infrared Training Center, 2015). For opaque surfaces this becomes

$$a + r = 1.$$

For the body to be at equilibrium, the received energy must be equal to the emitted energy, therefore

$$a = \varepsilon,$$

where the value of emissivity, ε , for a surface represents the surfaces ability to emit radiation. Furthermore, this leads to the relationship

$$\varepsilon = 1 - r,$$

between emissivity and reflectivity. Note that emissivity values range from 0 to 1, with 0 being a perfect reflector and 1 being a perfect emitter (black-body).

The angular dependence of emissivity for general materials is shown in Figure 1. This figure shows that the emissivity does not vary much for shallow angles but changes rapidly when viewing objects nearly edge on. Additionally, the behavior is quite different for conductors and non-conductors, the former showing a brief increase before dropping near 90 degrees, while the latter shows a strong drop-off near 90 degrees.

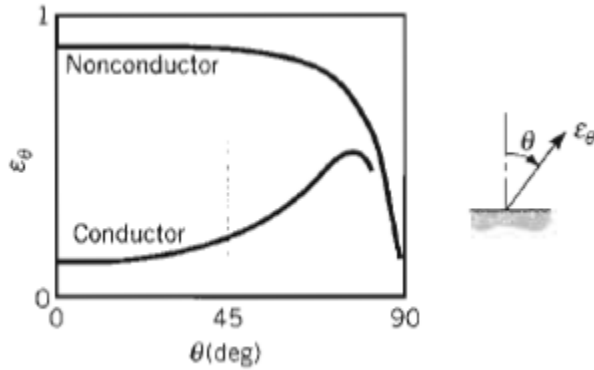


FIGURE 12.16
Representative directional distributions of the total, directional emissivity.

Figure 1. Variation of emissivity with angle for typical conductors (e.g. metals) and non-conductors (e.g. plastics) (Incropera & DeWitt, 2002).

Lastly, Table 1 shows emissivity for common materials. Most metals (conductors) have very low emissivity values, while plastics (non-conductors) have high emissivity values around 0.90-0.97. The values can be altered by polishing or roughening, hence the measured value for a unique surface is often the most accurate.

Surface/Material	Emissivity
Aluminum Foil	0.04
Aluminum Polished	0.04-0.06
Aluminum Black Anodized	0.85
Copper Polished	0.02
Gold polished	0.018
Carbon Charcoal Powder	0.96
Teflon (PTFE)*	0.85
PVC Dull Structured	0.94

Table 1. Emissivity values for various common engineering materials. Note that the metals (conductors) have very low emissivity values, while the plastics (non-conductors) have high emissivity values. Values are normal emissivity from Infrared Training Center, 2015, whereas *the value of Teflon is total hemispherical emissivity from Incropera & DeWitt, 2002.

Apparatus

Eight different additively manufactured samples were produced as emissivity sample coupons. The samples are 2in X 2in with 0.25in thickness. These coupons were produced with a layer height of 0.2mm and solid infill. Two coupons were produced for each material, one printed

vertically (one long direction upward) and one printed horizontally (with short direction upward).

Emissivity measurements were taken using a Gier-Dunkle reflectometer to first measure a number of samples of the reflectivity for each coupon. The emissivity was then calculated as $\varepsilon = 1 - r$. The angular dependence of the samples was then measured by placing the samples on a thermoelectric heater and recording the surface temperatures using a FLIR SC8300 MWIR infrared camera.

Procedure

Normal emissivity measurements were taken with the Gier-Dunkle reflectometer using the standard procedure for that equipment. These values are subsequently used for the 0 degree values of the angular dependence measurements. To take the angular dependence measurements, the camera is first aligned to the hot-plate as well as possible using a square running between the camera lens and the front edge of the hot-plate. Then a number of angles from 0 to 80 degrees were drawn on the surface as alignment targets. The hot-plate was allowed to stabilize at its set-point of 30C. Then the sample coupons were placed on the hot-plate and allowed to come to a steady-state (or nearly steady-state) temperature. Once this occurs, the sample is quickly marched through each angle and photographed, with care being exercised to minimize operator contact.

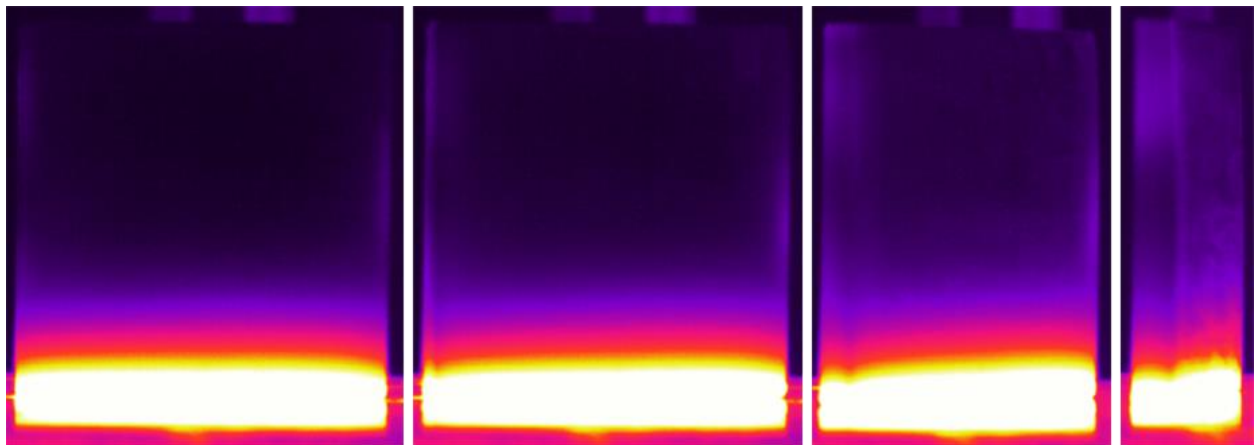


Figure 2. Infrared images of a sample at 0, 20, 50, and 80 angular degrees (from left to right).

Results

Table 2 shows the measured values of emissivity from the Gier-Dunkle reflectometer. These values are approximately 0.92 for all of the additively manufactured materials except the conductive PLA. This value puts these plastics in the range described in Table 1. Additionally, the conductive PLA has a lower emissivity which is consistent with the presence of a conductive component in the plastic. Table 3 shows a key to the sample orientation relative to the applied

numbers. There is no observed change for most samples for different build orientations. The uPrint material exhibits a difference, however this is within the error of the instrument used.

Material	average ϵ	Material	average ϵ
Gold	0.014	cPLA Sample1	0.883
Black	0.923	cPLA Sample2	0.897
Red ABS Sample 1	0.919	Gray PLA Sample 1	0.923
Red ABS Sample 2	0.917	Gray PLA Sample 2	0.916
uPrint ABS Sample 1	0.917	Natural PLA Sample 1	0.921
uPrint ABS Sample 2	0.902	Natural PLA Sample2	0.919

Table 2. Emissivities measured using the Gier- Dunkle reflectometer (Reid, 2016).

Material Name	Orientation	Material Name	Orientation
Gold	-	cPLA Sample1	Horizontal Top
Black	-	cPLA Sample2	Vertical
Red ABS Sample 1	Horizontal Bottom	Gray PLA Sample 1	Vertical
Red ABS Sample 2	Vertical	Gray PLA Sample 2	Horizontal Top
uPrint ABS Sample 1	Vertical	Natural PLA Sample 1	Vertical
uPrint ABS Sample 2	Horizontal Bottom	Natural PLA Sample2	Horizontal Bottom

Table 3. Orientation key to number descriptors for sample coupons.

Figure 3 shows the apparent temperature (uncompensated temperature from the FLIR with settings of $\epsilon=1$, $D=0$). The trends compare well with each other, with the exception of one of the uPrint samples. However this deviation is only minor. Figure 4 shows the change in temperature over the experiment. The curves nearly collapse when plotted this way, and show a consistent rise and then a drop off at large angles. It is likely that the samples are not at steady state temperature and are continuing to heat over the test, or a small amount of heat from the operator is raising the temperature.

Figure 5 shows the emissivity of the samples calculated by setting the 0 degree value to that given in Table 2. The emissivity for the other angles are then set by matching the resulting temperature to the value at 0 degrees. However, since the sample seems to be heating with time, this results in some non-physical emissivity values. This results in an angular dependence of emissivity that is similar to that shown in Figure 1 for conductors and non-conductors.

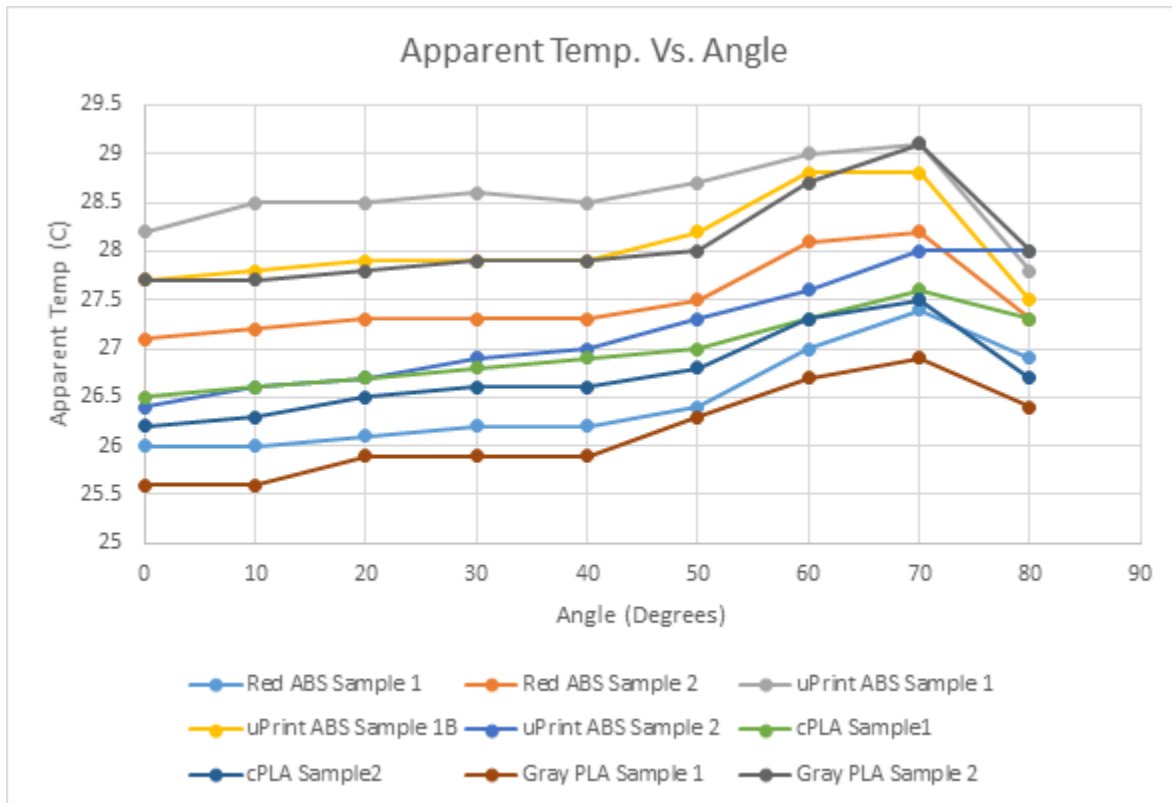


Figure 3. Raw apparent temperature measurements versus angle for each emissivity sample coupon.

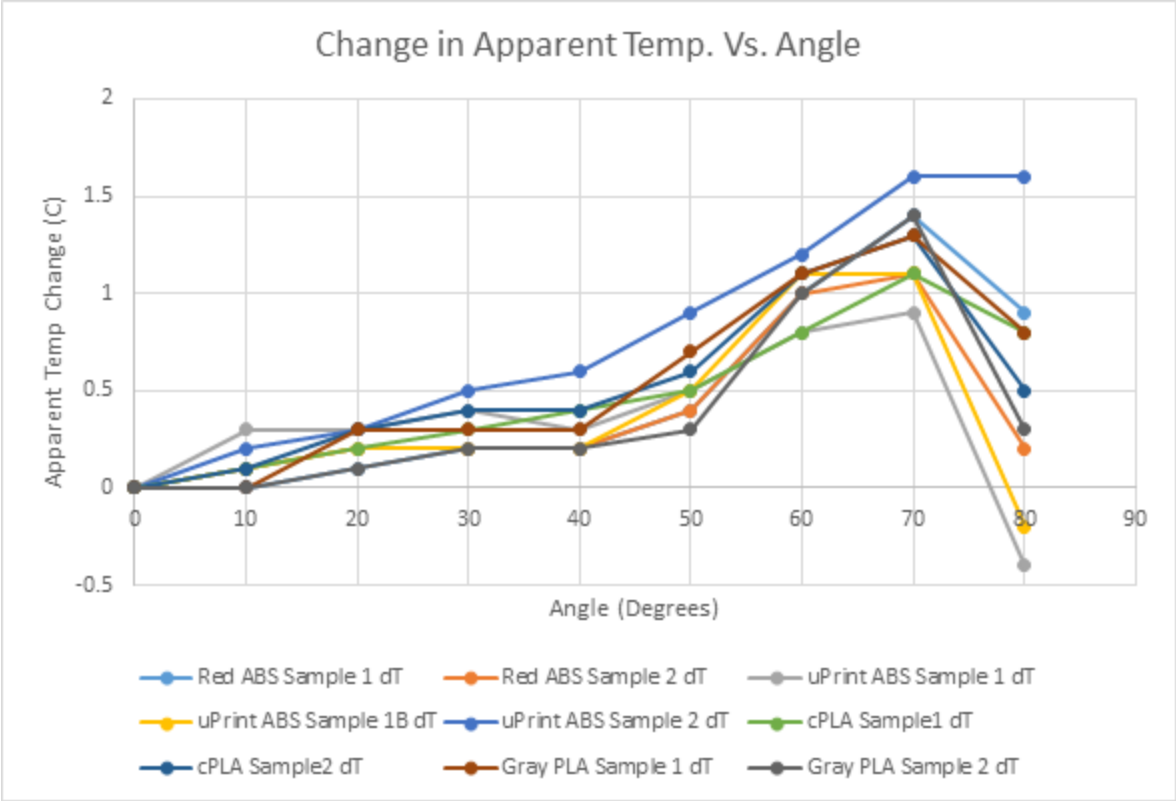


Figure 4. Change in apparent temperature measurements to eliminate contribution of initial temperature on data profiles.

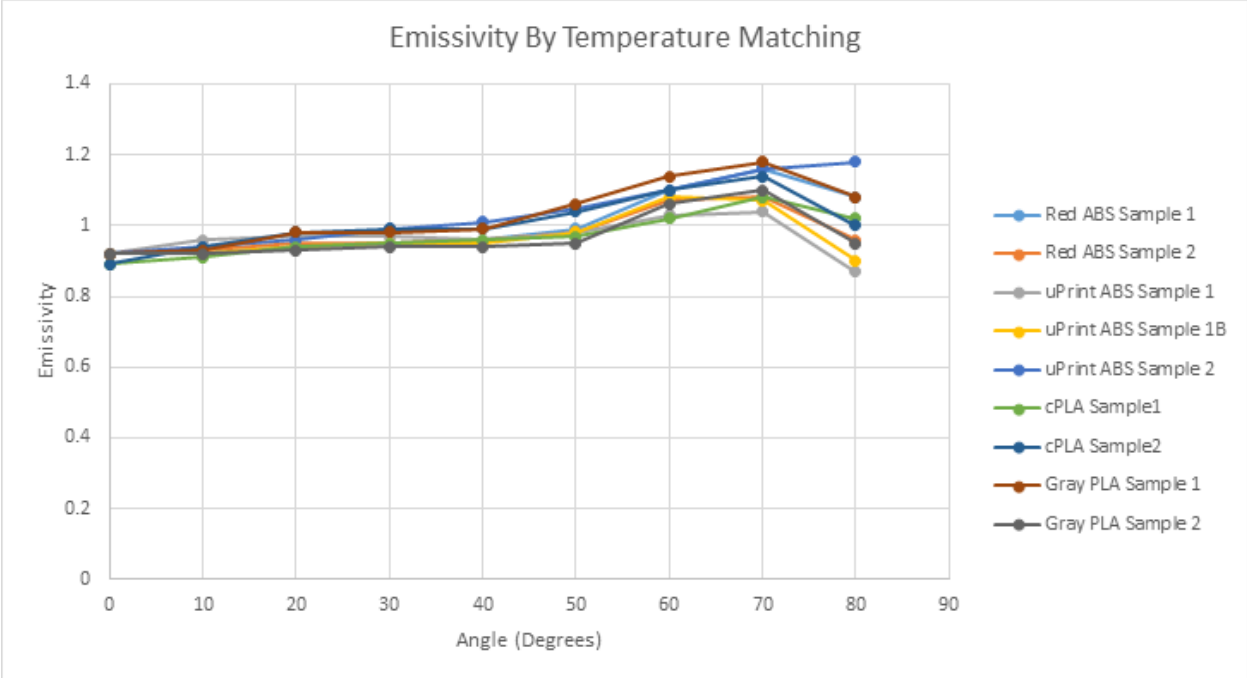


Figure 5. Emissivity calculated by setting the 0 degree value to that from Table 2, then adjusting the emissivity at the remaining angles until the temperature matches. This technique is easily influenced by temperature fluctuations.

Conclusions

The emissivity values of common 3D printing materials such as ABS and PLA fall in a typical range for plastics, and have the measured value of approximately 0.92. This value appears to be independent of the coloring of the material, and the surface finish imparted by different 3D printers. We anticipate however that this surface finish may have an effect if it can be changed drastically from the current “as printed” conditions. Adding a conductive material to the filament appears to cause a decrease in the emissivity of the surface despite the high emissivity of carbon (the dopant in the used filament). Lastly, the emissivity does not change much for shallow angles less than 40 degrees, and drops off dramatically after 70 degrees. Hence, for good quality IR temperature measurements, shallow angles should be avoided, and for the highest accuracy, observation angles should be kept below 40 degrees.

References

- Incropera, F. P., & DeWitt, D. P. (2002). *Fundamental of Heat and Mass Transfer*. Hoboken: John Wiley and Sons.
- Infrared Training Center. (2015). *Level I Thermography*. Nashua: ITC.
- Reid, R. S. (2016). Emissivity Measurement (Personal Communication). LANL AET-1.

Appendix A

Sample	Gold	Black	Red ABS Sample 1	Red ABS Sample 2	uPrint ABS Sample 1	uPrint ABS Sample 2	cPLA Sample1	cPLA Sample2	Gray PLA Sample 1	Gray PLA Sample 2	Natural PLA Sample 1	Natural PLA Sample2
1	0.985	0.08	0.08	0.083	0.084	0.098	0.106	0.102	0.078	0.076	0.077	0.078
2	0.987	0.072	0.081	0.08	0.082	0.097	0.109	0.101	0.077	0.079	0.076	0.076
3	0.986	0.076	0.081	0.085	0.082	0.097	0.109	0.104	0.077	0.081	0.076	0.078
4	0.988	0.078	0.081	0.085	0.082	0.097	0.108	0.105	0.077	0.085	0.077	0.077
5	0.988	0.078	0.08	0.082	0.082	0.095	0.115	0.102	0.075	0.086	0.08	0.076
6	0.987	0.079	0.081	0.082	0.081	0.097	0.118	0.102	0.075	0.087	0.08	0.078
7	0.984	0.076	0.08	0.085	0.083	0.098	0.118	0.103	0.078	0.085	0.08	0.082
8	0.985	0.077	0.078	0.084	0.083	0.097	0.119	0.103	0.077	0.087	0.08	0.084
9	0.987	0.077	0.08	0.084	0.084	0.099	0.12	0.102	0.079	0.086	0.081	0.084
10	0.987	0.074	0.081	0.083	0.084	0.099	0.125	0.105	0.08	0.085	0.082	0.084
11	0.987	0.076	0.084	0.083	0.082	0.099	0.128	0.103	0.079	0.085	0.08	0.085
12	0.983	0.082	0.083	0.082	0.084	0.099	0.128	0.101	0.078	0.085	0.083	0.085
average r	0.986	0.077	0.081	0.083	0.083	0.098	0.117	0.103	0.078	0.084	0.079	0.081
average ϵ	0.014	0.923	0.919	0.917	0.917	0.902	0.883	0.897	0.923	0.916	0.921	0.919

Table 4. Raw reflectivity data from the Gier-Dunkle reflectometer.